

—Original—

Involvement of B cells in the pathophysiology of β -aminopropionitrile-induced thoracic aortic dissection in mice

Yanxiang GAO¹⁾, Zhizhi WANG²⁾, Jianqiao ZHAO³⁾, Weiliang SUN⁴⁾, Jing GUO⁴⁾, Zufang YANG³⁾, Yimin TU²⁾, Changan YU⁵⁾, Lin PAN⁴⁾ and Jingang ZHENG^{1,2,3)}

¹⁾Department of Cardiology, China-Japan Friendship Hospital, 2 Yinghua Dongjie, Chaoyang District, Beijing 100029, China

²⁾Department of Cardiology, China-Japan Friendship School of Clinical Medicine, Peking Union Medical College, Chinese Academy of Medical Sciences, Beijing, 100029, China

³⁾Department of Cardiology, Peking University China-Japan Friendship School of Clinical Medicine, Beijing, 100029, China

⁴⁾Biomedical Experimental Research, Institute of Clinical Medicine, China-Japan Friendship Hospital, 2 Yinghua Dongjie, Chaoyang District, Beijing 100029, China

⁵⁾Central Laboratory of Cardiovascular Disease, China-Japan Friendship Hospital, 2 Yinghua Dongjie, Chaoyang District, Beijing 100029, China

Abstract: Thoracic aortic dissection (TAD) is a life-threatening disease that is characterized by an inflammatory response. Innate and cellular immunity has long been known to be involved in TAD, but the role of humoral immunity in the pathophysiology of TAD remains unknown. We administered the lysyl oxidase inhibitor β -aminopropionitrile (BAPN; 1 g/kg/day) in 3-week-old male C57BL/6J mice for 4 weeks to establish an animal model of TAD. Animals that died were immediately dissected. Animals that survived were sacrificed on days 7, 14, and 28 after BAPN challenge. The incidence and rupture rates of BAPN-induced TAD were 90% (9/10) and 70% (7/10), respectively, at 28 days. Victoria blue-nuclear fast red staining of aortic tissue revealed elastic lamellae destruction and the formation of a false lumen in the BAPN group. Hematoxylin-eosin staining revealed the infiltration of both plasmacytoid mononuclear cells and polymorphonuclear inflammatory cells in TAD tissues. Enzyme-linked immunosorbent assay and immunohistochemistry indicated that plasma immunoglobulin M (IgM) and IgG were elevated at 7, 14, and 28 days, and CD19-positive B cells infiltrated into the adventitia of aortic tissue in BAPN-treated mice. The transcriptional analysis showed an increase in the expression of B cell receptor signaling-associated genes. These results indicate that B cells and immunoglobulins might participate in the pathogenesis of TAD, suggesting that humoral immunity may be a possible therapeutic target for TAD.

Key words: β -aminopropionitrile, B cells, immunoglobulins, thoracic aortic dissection

(Received 8 November 2018 / Accepted 3 March 2019 / Published online in J-STAGE 29 March 2019)

Corresponding author: J. Zheng. e-mail: mdjingangzheng@163.com

Supplementary Figures: refer to J-STAGE: <https://www.jstage.jst.go.jp/browse/exanim>



This is an open-access article distributed under the terms of the Creative Commons Attribution Non-Commercial No Derivatives (by-nc-nd) License <<http://creativecommons.org/licenses/by-nc-nd/4.0/>>.

Introduction

Thoracic aortic dissection (TAD) is one of the most dangerous forms of vascular disease, with high mortality rates that are attributable to potentially fatal complications [5]. Epidemiological studies have shown that the incidence of aortic dissection ranges between 2.6 and 3.5 cases per 100,000 people per year [4, 10], which has increased in recent years [15]. Although examination techniques, surgical repair, and intravascular stent application improve the prognosis of aortic dissection patients, treatment efficacy remains unsatisfactory for some patients. To date, no specific early diagnostic tool or effective therapeutic drug is available because the mechanisms that underlie aortic dissection remain unclear. Therefore, elucidating the molecular causes and pathobiology of TAD is needed, in addition to identifying novel therapeutic targets.

The histopathological features of TAD include elastin fragmentation and degeneration and infiltration of the aortic media and adventitia by inflammatory cells. Inflammation is an essential characteristic of TAD and contributes to the fragmentation and depletion of elastic fibers, thereby leading to the formation of TAD [8, 23]. The suppression of inflammatory signaling has been shown to effectively prevent the progression of TAD in animal models [1, 20]. Human TAD tissue showed the early infiltration of inflammatory cells, including neutrophils, macrophages, T cells, and mast cells, which participate in the pathogenesis of TAD [22]. A series of studies have shown that B cells promote abdominal aortic aneurysm by producing immunoglobulins (Igs), which can induce degradation of the aortic wall by activating complementary pathways in a mouse model of elastase-induced aortic aneurysm [25, 26]. However, whether B cells are involved in the pathogenesis TAD remains unknown.

In the present study, we established a mouse model of TAD by administering β -aminopropionitrile (BAPN), which inhibits the activity of lysyl oxidase, an important enzyme for the organization, cross-linking, and maturation of extracellular matrix proteins (e.g., collagen and elastin). To explore the role of humoral immunity in the development of TAD, we evaluated plasma Ig levels, B cells in dissection tissue, and the expression of B cell receptor signaling-associated genes in the aorta.

Materials and Methods

Animals

Sixty 3-week-old male C57BL/6J mice were procured from Vital River Laboratory Animal Technology Co., Ltd., (Beijing, China). The animals were housed at 26–28°C and 40–60% humidity with a 12 h/12 h light/dark cycle under specific pathogen-free conditions. The animals were fed standard chow. After being matched for both body weight and blood pressure, the animals were randomized into two groups: control group and BAPN group (n=10/group for each time point). The BAPN group received BAPN (1.0 g/kg/day, Sigma, St. Louis, MO, USA), dissolved in drinking water as previously described [7, 11]. The control group received normal drinking water. During the experimental period, changes in body weight and systolic blood pressure were monitored, and deaths were observed. Animals that died were immediately dissected. Animals that survived were sacrificed on days 7, 14, and 28 after BAPN treatment by an intraperitoneal injection of sodium pentobarbital (200 mg/kg). The aortas were isolated under a dissecting microscope. In the model of BAPN-induced TAD, aortic dissection occurred mainly in the thoracic aorta (ascending aorta and descending aorta), defined as disruption of the medial layer of the aortic wall, resulting in separation of the aortic wall layers and the subsequent formation of a true lumen and a false lumen.

The animal care and procedures were approved by the China-Japan Friendship Hospital Animal Welfare and Ethics Committee (protocol no. 160109), which meets the United States National Institutes of Health guidelines for the care and use of laboratory animals (revised 2011) and complies with the animal use ethics checklist set forth by Experimental Animals.

Blood pressure measurement

Systolic blood pressure and heart rate were measured in conscious, restrained mice using a noninvasive computerized tail-cuff system (Softron Biotechnology, Beijing, China) every week, beginning 1 day before BAPN administration. The animals were habituated to the device before measuring blood pressure to ensure accurate measurements. Blood pressure was calculated for each mouse as the average of five separate measurements in each session.

Histology and immunohistochemistry

Paraformaldehyde-fixed aortic tissue was embedded in paraffin and processed, and 4 μ m sections were stained with hematoxylin-eosin or Victoria blue-nuclear fast red. Additional sections were immunostained using an indirect horseradish peroxidase immunoperoxidase method and specific antibody for CD19 antigen (Abcam, Cambridge, MA, USA). Negative controls for immunostaining consisted of replacing the primary antibody with an equivalent concentration of irrelevant rabbit polyclonal antibody. At least three different specimens were analyzed. The aortic tissue staining results were analyzed using ImageJ image analysis software.

Enzyme-linked immunosorbent assay

The concentrations of immunoglobulin M (IgM) and IgG in blood samples were analyzed using mouse-specific IgM and IgG enzyme-linked immunosorbent assay (ELISA) kits (Bethyl Laboratories, Montgomery, TX, USA) according to the manufacturer's instructions. Absorbance was read at 450 nm using a Multi-Mode Microplate Reader (SpectraMax M2, MTX Lab Systems, Bradenton, FL, USA).

RNA sequencing and data analysis

The mouse aortas were collected for total RNA extraction and further analysis. The cleaved RNA fragments were then reverse-transcribed to create the final cDNA library in accordance with the protocol for the mRNA Seq sample preparation kit (Illumina, San Diego, CA, USA). The average insert size for the paired-end libraries was 300 bp (\pm 50 bp). We then performed paired-end sequencing on an Illumina HiSeq 4000 (LC Sciences, Santiago, CA, USA) according to the manufacturer's protocol. Differential and significant gene expression analyses were performed using gene-level FPKM (Fragment Per Kilobase of exon model per Million mapped reads) expression levels. Genes were selected using the criteria of an absolute expression level >1 FPKM in the samples. Significant differentially expressed genes of each pairwise comparison were selected ($P < 0.05$, \log_2 [fold change] > 1 or \log_2 [fold change] < -1). Gene lists of relative enrichments for various ontology associations were determined using the Gene Ontology (GO) database.

Quantitative real-time polymerase chain reaction

Total RNA from aortic tissue was isolated with TRIzol

reagent (Applygen Technologies, Beijing, China) according to the manufacturer's protocol. cDNA was synthesized from 1.5 μ g of total RNA using the All-in-one First-Strand cDNA Synthesis Kit (Abcam, Cambridge, MA, USA). Real-time polymerase chain reaction (PCR) was performed using TransStart Green qPCR Supermix (TransGen Biotech, Beijing, China). All of the samples were amplified in duplicate. The primer sequences for the amplification of *Bcl6*, *Fos*, and *Gapdh* were the following: *Bcl6* (forward, AAATCTGTGGCACTC-GCTTCC; reverse, GGTATTGCACCTTGGTGTGG), *Fos* (forward, CCAGTCAAGAGCATCAGCAA; reverse, TAAGTAGTGCAGCCCGGAGT), and *Gapdh* (forward, TCTGAGGGCCCACTGAAG; reverse, AGGGTTTCTTACTCCTTGGAGG). The PCR runs and analyses were performed using the ABI Prism 7500 Sequence Detector and software (Applied Biosystems, Thermo Fisher, Wilmington, DE, USA).

Statistical analysis

All of the data are expressed as mean \pm SEM or representative raw data. For the statistical comparisons, we first determined whether the data were normally distributed. Similar variances were checked among normally distributed data, followed by Student's *t*-test for two-group comparisons and analysis of variance (ANOVA) for multiple-group comparisons if tests of similar variances were passed. The χ^2 test was used to compare the occurrence of mouse TAD. Kaplan-Meier survival curves were generated to analyze the survival percentage in the vehicle- and BAPN-treated groups. In all cases, values of $P < 0.05$ were considered statistically significant. All of the statistical analyses were performed using Prism 5.0 software (GraphPad, San Diego, CA, USA).

Results

Plasma IgM and IgG levels increased in BAPN evoked TAD mouse model

To investigate whether the humoral immune system is involved in the pathogenesis of TAD, we first established a mouse model of TAD by administering BAPN (1 g/kg/day) in 3-week-old male C57BL/6J mice for 4 weeks. The mice developed TAD and began to die from dissecting aneurysm rupture and thoracic hemorrhage 14 days after BAPN treatment (Fig. 1A). During the 4-week time course of BAPN challenge, the mortality and incidence of TAD in the BAPN group were 70%

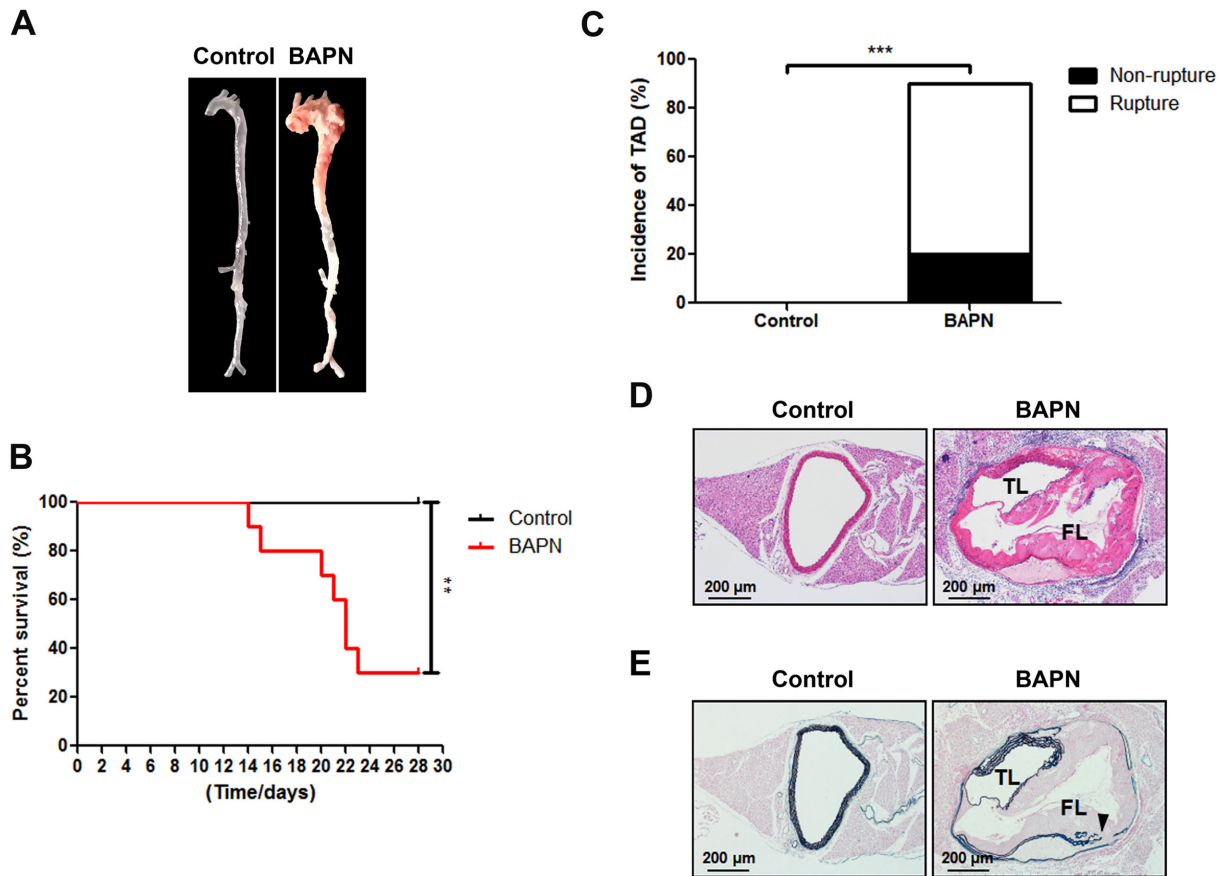


Fig. 1. β -aminopropionitrile (BAPN)-induced thoracic aortic dissection formation in mice. (A) Representative excised aortas that show that lesions formed in mice that were challenged with BAPN on day 28. (B) Survival curves were significantly worse in BAPN-challenged mice than in control mice. (C) Incidence of thoracic aortic dissection and rupture rate in mice 28 days after BAPN administration. (D, E) Representative histological sections of aortas that were stained with hematoxylin-eosin (D) and Victoria blue-nuclear fast red (E) 28 days after BAPN challenge. Obvious collapse of the elastic lamina (black arrowheads, elastic lamina fracture) and false lumen formation occurred in the BAPN group. $n=10/\text{group}$. $**P<0.01$, $***P<0.001$. FL, false lumen; TL, true lumen; TAD, thoracic aortic dissection.

(7/10) and 90% (9/10), respectively (Figs. 1B and C). No mice in the control group developed TAD or died. Histological examination of the aortas using hematoxylin-eosin staining (Fig. 1D) and Victoria blue-nuclear fast red staining (Fig. 1E) indicated false lumen formation, severe degeneration, and collapse of the elastic lamina in the BAPN group. No significant differences in body weight or systolic blood pressure were found between the control group and BAPN group (Supplementary Fig. S1). Plasma IgM and IgG levels were recorded 7, 14, and 28 days after BAPN challenge. As shown in Fig. 2, plasma IgM and IgG levels were persistently upregulated beginning in the initial stage of BAPN-induced TAD. The peak IgM level occurred on day 14, and the peak IgG level occurred on day 28.

B cells infiltrated TAD aortic tissues

Based on our finding that the levels of IgM and IgG, the major effector molecules of B cells, increased in TAD mice, we next examined the presence of B cells in TAD tissue samples. Hematoxylin-eosin staining indicated that numerous mononuclear and multinuclear inflammatory cells, including plasmacytoid cells, infiltrated the adventitia (Fig. 3A). Immunostaining with an antibody that was specific for B cells showed that CD19-positive B cells were present in adventitia of the aortic wall in BAPN-treated mice (Fig. 3B). In control mice (i.e., untreated mouse aorta), we found no B cells or plasmacytoid cells.

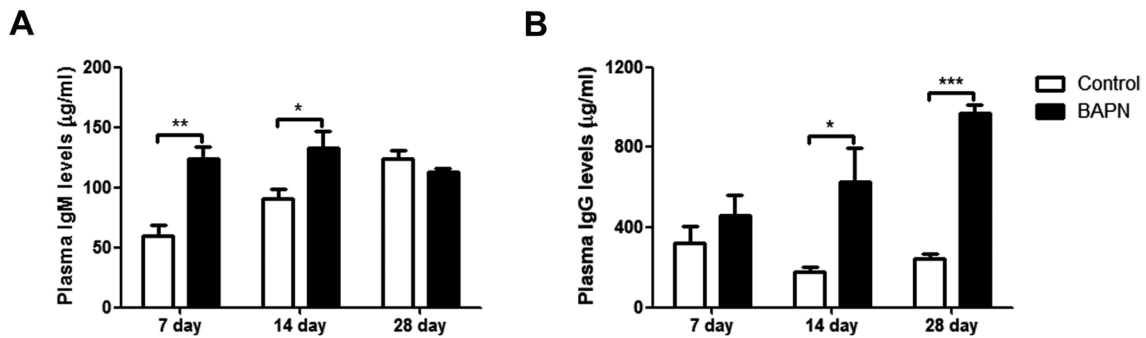


Fig. 2. Plasma levels of immunoglobulin M (IgM) and IgG were significantly higher in the β -aminopropionitrile (BAPN) group than in the control group. (A, B) Plasma levels of IgM (A) and IgG (B) in the control group and BAPN group 7, 14, and 28 days after BAPN administration. The data are expressed as mean \pm SEM. $n=10/\text{group}$. * $P<0.05$, ** $P<0.01$, *** $P<0.001$, compared with respective controls.

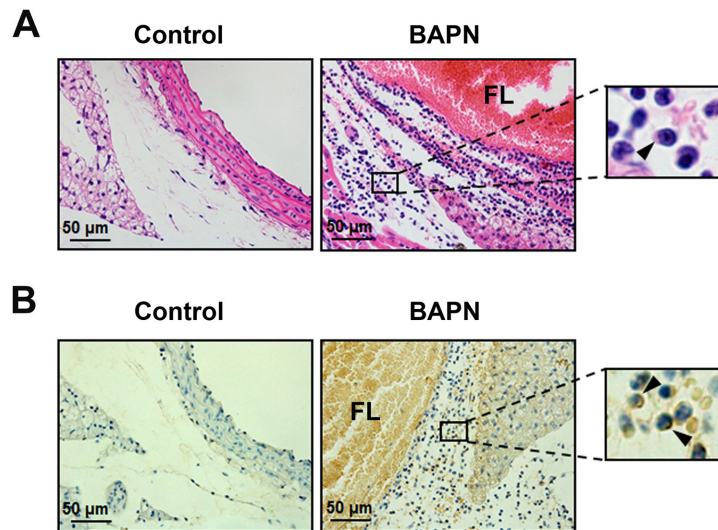


Fig. 3. B cells infiltrated aortic dissection tissues. (A) Representative histological sections of the aortas were stained with hematoxylin-eosin 28 days after β -aminopropionitrile (BAPN) challenge. The black arrowhead indicates plasmacytoid cells. (B) Representative images of immunohistochemical staining of CD19-positive cells in the aortic wall 28 days after BAPN administration. Black arrowhead indicates CD19-positive cells. $n=3/\text{group}$. FL, false lumen.

Involvement of B cell receptor signaling pathway in the pathogenesis of TAD

We performed RNA sequencing in mouse aortic tissues that were extracted 7 days after BAPN challenge to investigate the involvement of B cells in the pathogenesis of TAD. Among the 42,122 detected genes, the expression of 730 genes significantly increased or decreased ($P<0.05$, \log_2 [fold change] >1 or \log_2 [fold change] <-1) in BAPN-challenged aortas. The GO terms indicated functional annotations that clustered in “B cell receptor signaling pathway” and “antigen processing and

presentation.” These findings suggested that humoral immune responses were induced in the present mouse model of TAD. The hierarchical clustering analysis of gene expression patterns showed that a significant portion of these genes, such as *Cd19*, *Cd79b*, *Blnk*, *Ifitm1*, *Fos*, *Rac2*, and *Cd74*, were induced by BAPN challenge (Fig. 4A). We validated the transcriptional analysis results using real-time PCR and found that the mRNA expression of *Bcl6* and *Fos* was significantly upregulated in BAPN-challenged mice vs. control mice 7 days after BAPN administration (Figs. 4B and C). Addition-

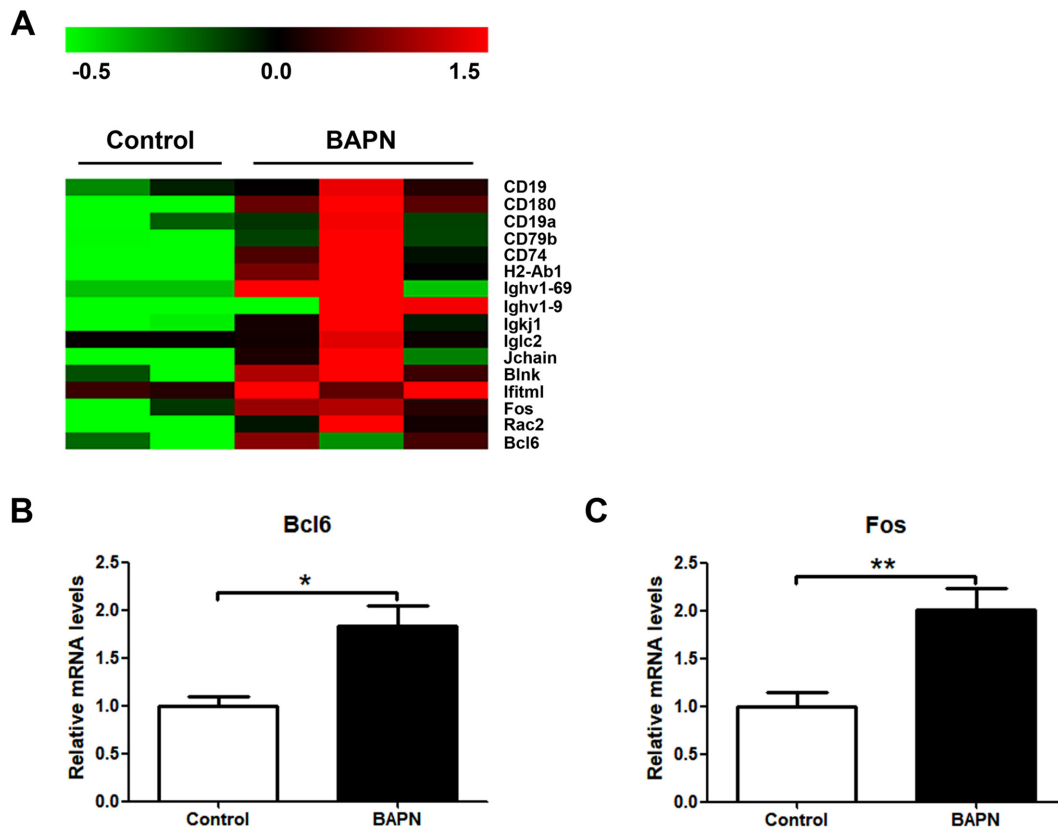


Fig. 4. Expression of genes related to B cell receptor signaling pathway increased in the β -aminopropionitrile (BAPN) group. (A) The results of the hierarchical clustering analysis of genes in the mouse aorta 7 days after BAPN treatment with the indicated annotations are shown by a heat map. After log conversion of the signal value, the distance from the median is shown in green, black, and red when lower, intermediate, and higher than those of the other samples, respectively, within a given gene. $n=2\sim3$ /group. (B, C) Analysis of *Bcl6* (B) and *Fos* (C) mRNA expression by real-time PCR in aortic tissues in the control and BAPN groups 7 days after BAPN administration. $n=5$ /group. * $P<0.05$, ** $P<0.01$, compared with control mice.

ally, the immunohistochemical results showed that CD19 expression levels in the aortic wall were higher in the BAPN group than in the control group (Fig. 3B). Altogether, these findings demonstrated the importance of B cells in the pathogenesis of TAD.

Discussion

The present study showed that B cells infiltrated into aortic dissection tissues, and plasma IgM and IgG levels significantly increased in the mouse model of BAPN-induced TAD. Moreover, the expression of genes that are associated with the B cell receptor signaling pathway increased in aortic tissues in BAPN-treated mice in the early stage of the pathogenesis of TAD. Therefore, B cells and Igs appear to play an important role in the progression of TAD.

Previous whole-genome sequencing in humans and genome engineering in mice showed that a loss-of-function mutation of lysyl oxidase causes aortic aneurysm and dissection because of insufficient elastin and collagen cross-linking in the aortic wall [9, 12]. The lysyl oxidase inhibitor BAPN inhibits the organization, cross-linking, and maturation of extracellular matrix proteins, induces medial degeneration of the aorta, and results in the formation of aorta dissection and aneurysm [7, 11]. In the present study, histology indicated that BAPN challenge mainly had a destructive effect on the structure of the proximal aorta, with no significant differences in the abdominal aorta, cephalic artery, or digestive tracts between the control and BAPN groups (Supplementary Figs. S2 and S3). Thoracic aortic aneurysm and dissection in both human and mouse occur most often in the ascending aorta. Mechanisms driving this

regional specificity have not been defined clearly. The distinct embryonic origins of smooth muscle cells in the thoracic aorta may explain these specific pathologic features, which is one facet of the many unknown features in the mechanisms of thoracic aortic aneurysm and dissection [18]. Furthermore, hematoxylin-eosin and Victoria blue-nuclear fast red staining showed no significant pathological changes in the aorta 1, 3, and 7 days after BAPN treatment. The collapse of the elastic lamina appeared in the thoracic aorta in the BAPN group at 14 days, and false lumen formation and severe collapse of the elastic lamina in the thoracic aorta were present in the BAPN group at 28 days (Supplementary Fig. S4). These results are consistent with mortality that is associated with ruptured aortic dissection in mice. The mice began to form aortic dissection and die at 14 days, and most of the mice developed TAD 28 days after BAPN treatment. Besides, the incidence of BAPN-induced TAD was correlated with the age of mice. Younger mice aged between 2 and 5 weeks were shown to be more susceptible to the effects of BAPN than mature mice [14]. BAPN induced elastin fragmentation, but not the formation of aortic aneurysms and dissections in adult mice [2]. Consequently, we developed the TAD animal model using 3-week-old mice with BAPN challenge. In summary, our mouse model of BAPN-induced TAD recapitulated pathophysiological conditions of aortic dissection in humans that is caused by mutations of lysyl oxidase. The present mouse model also has the advantages of a high incidence of TAD, relatively simple surgery, and good repeatability.

Several animal models of TAD have been described previously. In wildtype mice, TAD can be induced by BAPN administration and angiotensin II (Ang II) infusion alone or combined [1, 7, 11, 20] or a high-fat diet plus Ang II infusion [13]. In apolipoprotein E-deficient (ApoE^{-/-}) mice, TAD can be induced by the continuous infusion of Ang II [21]. No animal model can fully recapitulate all aspects of human TAD. Nonetheless, we found that B cells were involved in the development of TAD after BAPN challenge, which is consistent with previous reports that B cells infiltrated into aortic tissues in ApoE^{-/-} mice that were infused with Ang II and in acute aortic dissection patients [3, 17]. Moreover, the RNA sequencing and quantitative real-time PCR data showed that the expression of molecules that are related to the B cell receptor signaling pathway, including *Cd19*, *Cd79b*, *Blnk*, *Ifitm1*, *Bcl6*, *Fos*, *Rac2*, and *Cd74*, in-

creased in aortic tissues in mice that were treated with BAPN, which might due to the increasing number of B cells in aortic wall. These results indicated that B cells might play an important role in this disease. B cell-deficient muMT mice were reported to be protected from elastase-induced abdominal aortic aneurysm [26], and B cell depletion by anti-CD20 antibody abrogated the development of abdominal aortic aneurysm that was induced by Ang II in ApoE^{-/-} mice [19]. Further studies are required to elucidate the involvement of B cells in the pathogenesis of TAD using anti-CD20 antibody or muMT mice in different animal models of TAD.

Lymphocytes are a well-defined component of inflammation in many diseases and have been implicated as a contributing factor in vascular pathology, such as atherosclerosis and abdominal aortic aneurysm [16, 24]. The infiltration of B cells into abnormal aortic tissues may be important for antigen presentation and the continuous production of pathogenic cytokines and Igs, resulting in the activation of macrophages, mast cells, and complementary pathways in TAD tissue. In the present study, we found that plasma IgM and IgG levels began to increase in the early stage of TAD. The administration of exogenous polyclonal Igs was sufficient to promote interleukin-6 and matrix metalloproteinase-9 secretion in human abdominal aortic aneurysm tissue [6]. In the present study, elevated circulating Igs might have contributed to the maintenance of inflammation in mice with BAPN-induced TAD.

In conclusion, we found that B cells, Igs, and related signaling molecules were involved in the development of TAD. Further studies are required to delineate the mechanisms of B cell activation and Ig-mediated proinflammatory function in the context of TAD, which could lead to the identification of molecular targets for future diagnostic and therapeutic approaches.

Acknowledgments

This work was supported by the National Natural Science Foundation of China (no. 91639110, 81500326) and Beijing Natural Science Foundation (no. 7172195).

References

1. Anzai, A., Shimoda, M., Endo, J., Kohno, T., Katsumata, Y., Matsushashi, T., Yamamoto, T., Ito, K., Yan, X., Shirakawa, K., Shimizu-Hirota, R., Yamada, Y., Ueha, S., Shinmura, K., Okada, Y., Fukuda, K. and Sano, M. 2015. Adventitial

- CXCL1/G-CSF expression in response to acute aortic dissection triggers local neutrophil recruitment and activation leading to aortic rupture. *Circ. Res.* 116: 612–623. [Medline] [CrossRef]
2. Chen, J.Y., Tsai, P.J., Tai, H.C., Tsai, R.L., Chang, Y.T., Wang, M.C., Chiou, Y.W., Yeh, M.L., Tang, M.J., Lam, C.F., Shiesh, S.C., Li, Y.H., Tsai, W.C., Chou, C.H., Lin, L.J., Wu, H.L. and Tsai, Y.S. 2013. Increased aortic stiffness and attenuated lysyl oxidase activity in obesity. *Arterioscler. Thromb. Vasc. Biol.* 33: 839–846. [Medline] [CrossRef]
 3. del Porto, F., Proietta, M., Tritapepe, L., Miraldi, F., Koverech, A., Cardelli, P., Tabacco, F., de Santis, V., Vecchione, A., Mitterhofer, A.P., Nofroni, I., Amodeo, R., Trapolini, M. and Aliberti, G. 2010. Inflammation and immune response in acute aortic dissection. *Ann. Med.* 42: 622–629. [Medline] [CrossRef]
 4. Erbel, R., Aboyans, V., Boileau, C., Bossone, E., Bartolomeo, R.D., Eggebrecht, H., Evangelista, A., Falk, V., Frank, H., Gaemperli, O., Grabenwöger, M., Haverich, A., Jung, B., Manolis, A.J., Meijboom, F., Nienaber, C.A., Roffi, M., Rousseau, H., Sechtem, U., Sirnes, P.A., Allmen, R.S., Vrints, C.J., ESC Committee for Practice Guidelines. 2014. 2014 ESC Guidelines on the diagnosis and treatment of aortic diseases: Document covering acute and chronic aortic diseases of the thoracic and abdominal aorta of the adult. The Task Force for the Diagnosis and Treatment of Aortic Diseases of the European Society of Cardiology (ESC). *Eur. Heart J.* 35: 2873–2926. [Medline] [CrossRef]
 5. Evangelista, A., Isselbacher, E.M., Bossone, E., Gleason, T.G., Eusanio, M.D., Sechtem, U., Ehrlich, M.P., Trimarchi, S., Braverman, A.C., Myrmet, T., Harris, K.M., Hutchinson, S., O’Gara, P., Suzuki, T., Nienaber, C.A., Eagle, K.A., IRAD Investigators. 2018. Insights From the International Registry of Acute Aortic Dissection: A 20-Year Experience of Collaborative Clinical Research. *Circulation* 137: 1846–1860. [Medline] [CrossRef]
 6. Furusho, A., Aoki, H., Ohno-Urabe, S., Nishihara, M., Hirakata, S., Nishida, N., Ito, S., Hayashi, M., Imaizumi, T., Hiromatsu, S., Akashi, H., Tanaka, H. and Fukumoto, Y. 2018. Involvement of B Cells, Immunoglobulins, and Syk in the Pathogenesis of Abdominal Aortic Aneurysm. *J. Am. Heart Assoc.* 7: 7. [Medline] [CrossRef]
 7. Gao, Y.X., Liu, Y.T., Zhang, Y.Y., Qiu, J.J., Zhao, T.T., Yu, C.A. and Zheng, J.G. 2018. [Establishment of β -aminopropionitrile-induced aortic dissection model in C57Bl/6J mice]. *Zhonghua Xin Xue Guan Bing Za Zhi* 46: 137–142. [Medline]
 8. Goldfinger, J.Z., Halperin, J.L., Marin, M.L., Stewart, A.S., Eagle, K.A. and Fuster, V. 2014. Thoracic aortic aneurysm and dissection. *J. Am. Coll. Cardiol.* 64: 1725–1739. [Medline] [CrossRef]
 9. Guo, D.C., Regalado, E.S., Gong, L., Duan, X., Santos-Cortez, R.L., Arnaud, P., Ren, Z., Cai, B., Hostetler, E.M., Moran, R., Liang, D., Estrera, A., Safi, H.J., Leal, S.M., Bamshad, M.J., Shendure, J., Nickerson, D.A., Jondeau, G., Boileau, C., Milewicz, D.M., University of Washington Center for Mendelian Genomics. 2016. LOX Mutations Predispose to Thoracic Aortic Aneurysms and Dissections. *Circ. Res.* 118: 928–934. [Medline] [CrossRef]
 10. Hiratzka, L.F., Bakris, G.L., Beckman, J.A., Bersin, R.M., Carr, V.F., Casey, D.E. Jr., Eagle, K.A., Hermann, L.K., Isselbacher, E.M., Kazerooni, E.A., Kouchoukos, N.T., Lytle, B.W., Milewicz, D.M., Reich, D.L., Sen, S., Shinn, J.A., Svensson, L.G., Williams, D.M., American College of Cardiology Foundation/American Heart Association Task Force on Practice Guidelines, American Association for Thoracic Surgery, American College of Radiology, American Stroke Association, Society of Cardiovascular Anesthesiologists, Society for Cardiovascular Angiography and Interventions, Society of Interventional Radiology, Society of Thoracic Surgeons, Society for Vascular Medicine. 2010. 2010 ACCF/AHA/AATS/ACR/ASA/SCA/SCAI/SIR/STS/SVM guidelines for the diagnosis and management of patients with Thoracic Aortic Disease: a report of the American College of Cardiology Foundation/American Heart Association Task Force on Practice Guidelines, American Association for Thoracic Surgery, American College of Radiology, American Stroke Association, Society of Cardiovascular Anesthesiologists, Society for Cardiovascular Angiography and Interventions, Society of Interventional Radiology, Society of Thoracic Surgeons, and Society for Vascular Medicine. *Circulation* 121: e266–e369. [Medline]
 11. Jia, L.X., Zhang, W.M., Zhang, H.J., Li, T.T., Wang, Y.L., Qin, Y.W., Gu, H. and Du, J. 2015. Mechanical stretch-induced endoplasmic reticulum stress, apoptosis and inflammation contribute to thoracic aortic aneurysm and dissection. *J. Pathol.* 236: 373–383. [Medline] [CrossRef]
 12. Lee, V.S., Halabi, C.M., Hoffman, E.P., Carmichael, N., Leshchiner, I., Lian, C.G., Bierhals, A.J., Vuzman, D., Mecham, R.P., Frank, N.Y., Stitzel, N.O., Brigham Genomic Medicine 2016. Loss of function mutation in LOX causes thoracic aortic aneurysm and dissection in humans. *Proc. Natl. Acad. Sci. USA* 113: 8759–8764. [Medline] [CrossRef]
 13. LeMaire, S.A., Zhang, L., Luo, W., Ren, P., Azares, A.R., Wang, Y., Zhang, C., Coselli, J.S. and Shen, Y.H. 2018. Effect of ciprofloxacin on susceptibility to aortic dissection and rupture in mice. *JAMA Surg.* 153: e181804. [Medline] [CrossRef]
 14. McCALLUM, H.M. 1958. Lathyrism in mice. *Nature* 182: 1169–1170. [Medline] [CrossRef]
 15. Mészáros, I., Mórocz, J., Szlávi, J., Schmidt, J., Tornóci, L., Nagy, L. and Szép, L. 2000. Epidemiology and clinicopathology of aortic dissection. *Chest* 117: 1271–1278. [Medline] [CrossRef]
 16. Moriya, J. 2019. Critical roles of inflammation in atherosclerosis. *J. Cardiol.* 73: 22–27. [Medline]
 17. Saraff, K., Babamusta, F., Cassis, L.A. and Daugherty, A. 2003. Aortic dissection precedes formation of aneurysms and atherosclerosis in angiotensin II-infused, apolipoprotein E-deficient mice. *Arterioscler. Thromb. Vasc. Biol.* 23: 1621–1626. [Medline] [CrossRef]
 18. Sawada, H., Chen, J.Z., Wright, B.C., Sheppard, M.B., Lu, H.S. and Daugherty, A. 2018. Heterogeneity of Aortic Smooth Muscle Cells: A Determinant for Regional Characteristics of Thoracic Aortic Aneurysms? *J. Transl. Int. Med.* 6: 93–96. [Medline] [CrossRef]

19. Schaheen, B., Downs, E.A., Serbulea, V., Almenara, C.C., Spinosa, M., Su, G., Zhao, Y., Srikakulapu, P., Butts, C., McNamara, C.A., Leitinger, N., Upchurch, G.R. Jr., Meher, A.K. and Ailawadi, G. 2016. B-Cell Depletion Promotes Aortic Infiltration of Immunosuppressive Cells and Is Protective of Experimental Aortic Aneurysm. *Arterioscler. Thromb. Vasc. Biol.* 36: 2191–2202. [[Medline](#)] [[CrossRef](#)]
20. Tieu, B.C., Lee, C., Sun, H., Lejeune, W., Recinos, A. 3rd., Ju, X., Spratt, H., Guo, D.C., Milewicz, D., Tilton, R.G. and Brasier, A.R. 2009. An adventitial IL-6/MCP1 amplification loop accelerates macrophage-mediated vascular inflammation leading to aortic dissection in mice. *J. Clin. Invest.* 119: 3637–3651. [[Medline](#)] [[CrossRef](#)]
21. Trachet, B., Piersigilli, A., Fraga-Silva, R.A., Aslanidou, L., Sordet-Dessimoz, J., Astolfo, A., Stampanoni, M.F., Segers, P. and Stergiopoulos, N. 2016. Ascending Aortic Aneurysm in Angiotensin II-Infused Mice: Formation, Progression, and the Role of Focal Dissections. *Arterioscler. Thromb. Vasc. Biol.* 36: 673–681. [[Medline](#)] [[CrossRef](#)]
22. Wu, D., Choi, J.C., Sameri, A., Minard, C.G., Coselli, J.S., Shen, Y.H. and LeMaire, S.A. 2013. Inflammatory Cell Infiltrates in Acute and Chronic Thoracic Aortic Dissection. *Aorta (Stamford)* 1: 259–267. [[Medline](#)] [[CrossRef](#)]
23. Wu, D., Shen, Y.H., Russell, L., Coselli, J.S. and LeMaire, S.A. 2013. Molecular mechanisms of thoracic aortic dissection. *J. Surg. Res.* 184: 907–924. [[Medline](#)] [[CrossRef](#)]
24. Zhang, L. and Wang, Y. 2015. B lymphocytes in abdominal aortic aneurysms. *Atherosclerosis* 242: 311–317. [[Medline](#)] [[CrossRef](#)]
25. Zhou, H.F., Yan, H., Bertram, P., Hu, Y., Springer, L.E., Thompson, R.W., Curci, J.A., Hourcade, D.E. and Pham, C.T. 2013. Fibrinogen-specific antibody induces abdominal aortic aneurysm in mice through complement lectin pathway activation. *Proc. Natl. Acad. Sci. USA* 110: E4335–E4344. [[Medline](#)] [[CrossRef](#)]
26. Zhou, H.F., Yan, H., Stover, C.M., Fernandez, T.M., Rodriguez de Cordoba, S., Song, W.C., Wu, X., Thompson, R.W., Schwaeble, W.J., Atkinson, J.P., Hourcade, D.E. and Pham, C.T. 2012. Antibody directs properdin-dependent activation of the complement alternative pathway in a mouse model of abdominal aortic aneurysm. *Proc. Natl. Acad. Sci. USA* 109: E415–E422. [[Medline](#)] [[CrossRef](#)]